*remote sensing*

MDPI

*Technical Note*

# Satellite Observations Reveal Declining Diatom Concentrations in the Three Gorges Reservoir: The Impacts of Dam Construction and Local Climate

**Menglan Gan [1,†], Lei Feng [2,†], Jingan Shao [1], Li Feng [3], Yao Wang [1], Meiling Liu [4], Ling Wu [4] and Botian Zhou [2,*]**

[1] School of Geography and Tourism, Chongqing Normal University, Chongqing 401331, China
[2] Chongqing Key Laboratory of Big Data and Intelligent Computing, Chongqing Institute of Green and Intelligent Technology, Chinese Academy of Sciences, Chongqing 400714, China
[3] Chongqing Collaborative Innovation Center of Big Data Application in Eco-Environmental Remote Sensing, Chongqing Academy of Ecological and Environmental Science, Chongqing 401147, China
[4] School of Information Engineering, China University of Geosciences, Beijing 100083, China
* Correspondence: zhoubotian@cigit.ac.cn
† These authors contributed equally to this work.

**Abstract:** An effective satellite observation system is developed to retrieve the diatom concentration in freshwater ecosystems that could be utilized for understanding aquatic biogeochemical cycles. Although the singular value decomposition-based retrieval model can reflect the complicated diatom dynamics, the spatial distribution and temporal trend in diatom concentration on a large scale, as well as its driving mechanism, remain prevalently elusive. Based on the Google Earth Engine platform, this study uses Sentinel-2 MultiSpectral Instrument imagery to track the comprehensive diatom dynamics in a large reservoir, i.e., the Three Gorges Reservoir, in China during the years 2019–2023. The results indicate that a synchronous diatom distribution is found between the upstream and downstream artificial lakes along the primary tributary in the Three Gorges Reservoir, and the causal relationships between the declining diatom trend and hydrological/meteorological drivers on the monthly and yearly scales are highlighted. Moreover, the Sentinel-derived diatom concentration can be used to ascertain whether the dominant algae are harmful during bloom periods and aid in distinguishing algal blooms from ship oil spills. This study is a significant step forward in tracking the diatom dynamics in a large-scale freshwater ecosystem involving complex coupling drivers.

**Keywords:** diatom concentration; Sentinel-2 multispectral instrument; singular value decomposition; Three Gorges Reservoir; Google Earth Engine

check for updates

Academic Editor: Hatim Sharif

Received: 13 December 2024
Revised: 7 January 2025
Accepted: 10 January 2025
Published: 16 January 2025

**Citation:** Gan, M.; Feng, L.; Shao, J.; Feng, L.; Wang, Y.; Liu, M.; Wu, L.; Zhou, B. Satellite Observations Reveal Declining Diatom Concentrations in the Three Gorges Reservoir: The Impacts of Dam Construction and Local Climate. *Remote Sens.* **2025**, *17*, 309. https://doi.org/10.3390/rs17020309

**Copyright:** © 2025 by the authors. Licensee MDPI, Basel, Switzerland. This article is an open access article distributed under the terms and conditions of the Creative Commons Attribution (CC BY) license (https://creativecommons.org/licenses/by/4.0/).

## 1. Introduction

Phytoplankton are responsible for half of global primary production, although they comprise only 0.2% of the photosynthetically active biomass globally [1–3]. In addition to forming the substance foundation of aquatic food webs, phytoplankton consist of basic nutrient fountainheads in marine and freshwater ecosystems [4–6]. Specifically, various algal species can achieve different ecological functions due to their biogeochemical roles in the phytoplankton community [7–9]. As a principal phytoplankton group, diatoms contribute to silica production in the global aquatic ecosystem, according to their morphological and physiological characteristics [10–12]. Moreover, as the largest phytoplankton group contributing to the carbon sink, diatoms effectively support carbon storage status in the ocean and inland waters [13–15]. Therefore, estimating the diatom concentration in the

phytoplankton community is important for evaluating the effects of diatom dynamics on the fishing industry, nutrient transfer, and carbon emission.

Methods such as electron microscopy, genetic analysis, and flow cytometry can be used to distinguish algal species and phytoplankton community structures. Furthermore, phytoplankton pigment chemotaxonomy with high-performance liquid chromatography (Shimadzu, Kyoto, Japan) or Phyto-PAM (WALZ, Würzburg, Germany) is widely applied to estimate the algal species concentration in an identified phytoplankton community structure [16–18]. However, in consideration of numerous restrictions for sampling activities in wide-region and long-term phytoplankton communities, developing in situ observation systems in relation to the diatom concentration represents technical and financial issues that can be obstructive in revealing the distribution, trends, and drivers of diatom concentration [19,20].

Recently, bio-optical technology improvements have led to the development of satellite sensors, which have become a cost-effective tool for representing the spatiotemporal variations in algal blooms, yet few remote sensing studies have followed the diatom issue, for which the concentration is commonly much lower than the chlorophyll concentration. Most previous efforts focus on detecting diatom dynamics on a large spatiotemporal scale, which can be difficult [21–23]. Nevertheless, there has been a growing interest in exploiting bio-optical features to retrieve the diatom concentration according to the dominant algal species, as well as the identification and targeting of the phytoplankton community properties based on the phytoplankton functional group or phytoplankton size structure [24]. Thus, the research on diatom concentration that is derived from remote sensing reflectance ($R_{rs}$) spectra is still insufficient.

The Singular Value Decomposition (SVD) model that is proposed, in combination with the water surface $R_{rs}$, is computed as a model of photosynthetic pigment concentration to describe diatom-dominated waters, which are accompanied by brown waters, compared to those that are dominated by other algal species; the model subsequently retrieves the diatom concentration in homogenization optical scenarios (e.g., marine ecosystems) [25]. The SVD model is not applied to track diatom dynamics considering the multiple effects of the hydrological and meteorological interaction processes, although it has been implemented repeatedly in coastal waters, the environment for which it was developed. Without appropriate validation, it is hard to determine the limitation and uncertainty associated with a model performance in heterogenization optical scenarios (e.g., freshwater ecosystems). Accordingly, the SVD model should be adjusted to adapt to local conditions before being applied in complex scenarios.

The Three Gorges Reservoir (TGR) in China can be considered as a complex scenario suffering from diatom-dominated phytoplankton groups over a given chlorophyll concentration [26–28]. Diatoms often dominate the phytoplankton community, particularly in the TGR's tributaries, with unique hydrological and meteorological interaction processes such as dammed rivers, strong sunshine, and abundant precipitation [29,30]. Consequently, as a mixed river–reservoir ecosystem, the TGR's tributaries can serve as excellent experimental sites to evaluate the SVD model's capability of tracking diatom dynamics in complex scenarios. By combining in situ and satellite observations, this study attempts to (1) reveal the spatial distribution and temporal trends in diatom concentration in a typical TGR tributary using Sentinel-2 MultiSpectral Instrument (MSI) imagery, and (2) elucidate the dam construction and local climate that drive the identified diatom dynamics, especially focusing on the quantitative analysis of temporal trends in the diatom concentration, in order to confirm whether hydrological or meteorological drivers dominate the diatom trend in a typical TGR tributary.

## 2. Materials and Methods

### *2.1. Study Area*

Considering the adaptability of the spatial resolution of satellite imagery to open waters, Lakes Hanfeng and Gaoyang, along the Xiaojiang River, which is a typical TGR tributary, were selected as the study area (Figure 1). These two artificial lakes were formed through the constructions of the Wuyang and Three Gorges Dams in May 2006 and May 2012, respectively [31]. Built as a pre-reservoir (or pre-dam) to specifically mitigate the negative impacts of the water level fluctuation zone along the Xiaojiang River, Lake Hanfeng, located approximately 40 km upstream from Lake Gaoyang, has a relatively stable water level (above 169 m since October 2017) [32]. Conversely, Lake Gaoyang, as a Yangtze River-connected lake, is jointly controlled by the Wuyang and Three Gorges Dams, and thus, its water level fluctuates between 145 m and 175 m [33]. Additionally, the two artificial lakes separated by the Wuyang Dam belong to the subtropical monsoon climate, with abundant precipitation throughout the year (daily mean precipitation is 3.44 mm), frequent cloud/fog in winter (number of days with sunshine duration of less than 1 h is 45.62 d), and a persistent heatwave in summer (daily mean air temperature reaches 26.93 °C) [34].

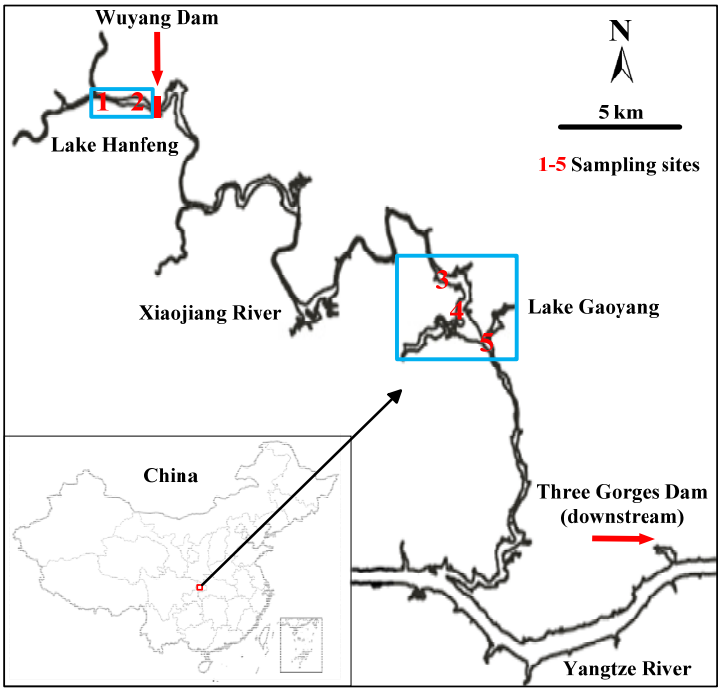



**Figure 1.** Location of Lakes Hanfeng and Gaoyang (indicated by blue boxes) along the Xiaojiang River in the TGR, China. The red numbers 1–5 represent the five sampling sites.

Accompanied by the tributary backwater formation since the TGR was constructed, algal blooms have been monitored along the Xiaojiang River due to industrial/agricultural wastewater and domestic sewage from the upstream tributary and the downstream Yangtze River [35]. With the succession of the phytoplankton community structure, there have been intermittent occurrences of diatom blooms in Lakes Hanfeng and Gaoyang since the diatom bloom along the Xiaojiang River was first reported in 2015 [26,36]. Therefore, the typical TGR tributary is suitable for large-scale studies on diatom dynamics affected by the interaction processes between dam construction and local climate.

### *2.2. In Situ Data Collection*

In the present study, ship surveys were performed 13 times from 2019 to 2023, covering different seasons and reservoir operation periods, and administered during 10:30 AM–11:30 AM,

in time with the satellite transit. Approximately 1 L of water sample was collected at a depth of 0.25 m with a polymethyl methacrylate sampler and then filtered through Whatman GF/C fiberglass filters with a pore size of 1.2 μm for the diatom concentration measurement. The diatom concentration was determined by measuring the chlorophyll concentration corresponding to diatoms using Phyto-PAM (WALZ, Würzburg, Germany) [37]. The diatom blooms are defined as states in which diatom concentration is greater than 10 μg/L [38]. The dominant species were identified with a CX31 microscope (Olympus, Tokyo, Japan), as shown in Figure 2 [39]. Moreover, water surface $R_{rs}$ spectra were recorded using a FieldSpec HandHeld 2 (ASD, Newark, NJ, USA) with a spectral resolution of 3 nm, spectral range of 350–1050 nm, and sampling interval of 1 nm [40].

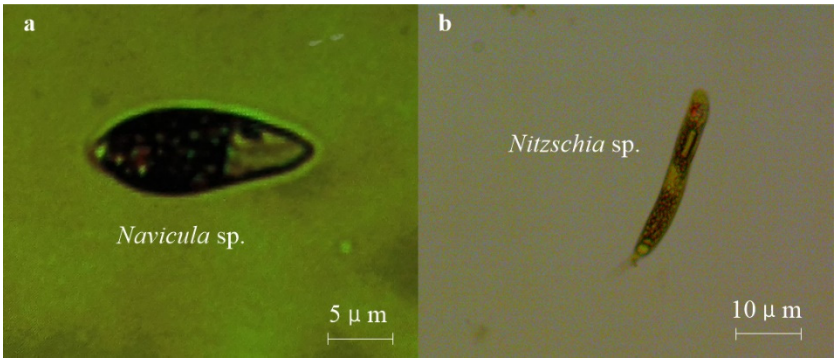



**Figure 2.** Microscopic photographs of (**a**) *Navicula* sp. and (**b**) *Nitzschia* sp.

During the investigation period of this study, hydrological (water level) and meteorological (air temperature, sunshine duration, and precipitation) drivers were considered. The water levels of Lakes Hanfeng and Gaoyang are the basis of the front and underwater levels of the Wuyang Dam, respectively. The air temperature, sunshine duration, and precipitation over the two artificial lakes, Hanfeng and Gaoyang, were obtained from the weather data in Kaizhou district and Yunyang county, respectively, provided by the Chongqing Municipal Bureau of Meteorology.

### *2.3. Satellite-Derived Diatom Concentration*

The Sentinel-2 MSI imagery was selected to replace the ocean and meteorological satellite geostationary ocean color imager, Seastar SeaWiFS, and Aqua/Terra moderate-resolution imaging spectroradiometer for retrieving diatom concentration in the narrow TGR tributary (narrowest river width is less than 50 m), because of the appropriate spectral, spatial, and temporal resolutions [41]. Accordingly, the Sentinel-2 MSI imagery was processed on the Google Earth Engine (GEE) platform, including radiometric calibration, atmospheric correction derived with Sen2Cor, and geometric rectification, to retrieve diatom concentrations in different seasons and cross-sections [42]. Once the MSI sensor began to stably output reliable data, a Sentinel-2 MSI imagery time series (from January 2019 to December 2023) with a revisit interval of 5 d became available for tracking diatom dynamics in Lakes Hanfeng and Gaoyang along the Xiaojiang River using five multispectral wavebands (i.e., coastal aerosol, blue, green, red, and red-edge wavebands, with spatial resolutions of 60 m, 10 m, 10 m, 10 m, and 10 m). Furthermore, ArcGIS was applied to resample the spatial resolution of multispectral imagery to 20 m and extract the water surface $R_{rs}$ spectra.

This study is based on SVD, which is a matrix factorization method widely used in linear algebra to extract the spectral features from standardized water surface $R_{rs}$ spectra and linearly fit the covariance matrix with the measured diatom concentration (Figure 3). Subsequently, the waveband combination and modeling dataset are continuously adjusted

to obtain the optimal fitting relationship and substitute it into the Sentinel-2 MSI imagery to extract the water surface $R_{rs}$ spectra to retrieve the diatom concentration [43]. However, the SVD-based retrieval model of diatom concentration is specifically designed for coastal waters, e.g., the East China Sea. There are many differences in the hydrological and meteorological conditions between the coastal and inland waters. Therefore, to achieve model application in freshwater ecosystems, the SVD model needs to be adaptively optimized for the local conditions. According to in situ $R_{rs}$ spectra and the measured diatom concentration in the Xiaojiang River, as well as the bicubic convolution interpolation and nearest neighbor method provided by the GEE platform, errors caused by spatiotemporal window and atmospheric correction can be overcome, and the red-edge waveband $R_{rs}$ is considered as an input, enabling the output of the SVD model to match the Sentinel-derived water surface $R_{rs}$ spectra in the typical TGR tributary and capture the corresponding diatom dynamics [44].

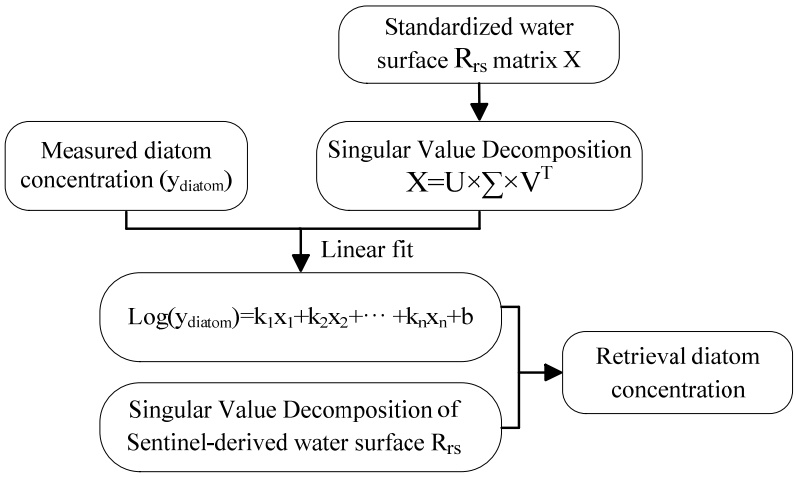



**Figure 3.** Flowchart of retrieval of diatom concentration.

### *2.4. Statistical Analysis Between Diatom Trends and Their Drivers*

To evaluate the causal correlation between hydrological/meteorological drivers and diatom concentration, the Pearson correlation coefficient *r* was employed. In this study, $|r| < 0.6$ and $|r| \geq 0.6$ indicate that the responses of the diatom trend to water level, air temperature, sunshine duration, and precipitation changes are limited and significant, respectively. Moreover, to quantify the relative contributions of dam construction and local climate to the diatom trend, a multiple general linear model was employed. In consideration of statistical significance, if the contribution $\geq$ 40%, it is considered as a dominant driver; if 20% $\leq$ contribution < 40% and $|r| \geq 0.6$, then it is also considered to strongly control the diatom trend. In addition, the change rate of the diatom trend is estimated using the slope of the fitting line.

## 3. Results

### *3.1. Spatial Distribution and Temporal Trend of Diatom Concentration*

An in situ dataset was collected using ship surveys during different seasons and reservoir operation periods over the past five years, which to some extent ensures the retrieval accuracy of the SVD model. A total of 43 cloud-free Sentinel-2 MSI images were provided between 2019 and 2023, fully covering the bloom period in the typical TGR tributary. Four of these images correspond to our ship surveys (sampling interval between in situ and satellite observations is less than 3 d, and weather conditions at the two sampling times are similar). According to the microscopic examination, the ranges of abundance and relative abundance of diatoms

matched with satellite observations are 13–1514 × $10^4$ cells/L and 3.2–74.57%, with the mean values of 106 × $10^4$ cells/L and 18.97%, respectively, indicating that algal samples cover various experimental scenarios such as no algal blooms, diatom blooms, and non-diatom blooms. As shown in Figure 4, the relationship between measured and retrieval diatom concentrations is inseparable ($r$ = 0.89, RMSE = 7.64 µg/L, and the $p$-level < 0.05), which is consistent with diatom studies in coastal waters, e.g., the Bohai Sea, Yellow Sea, and East China Sea [45], indirectly providing the SVD model with reliability in the typical TGR tributary.

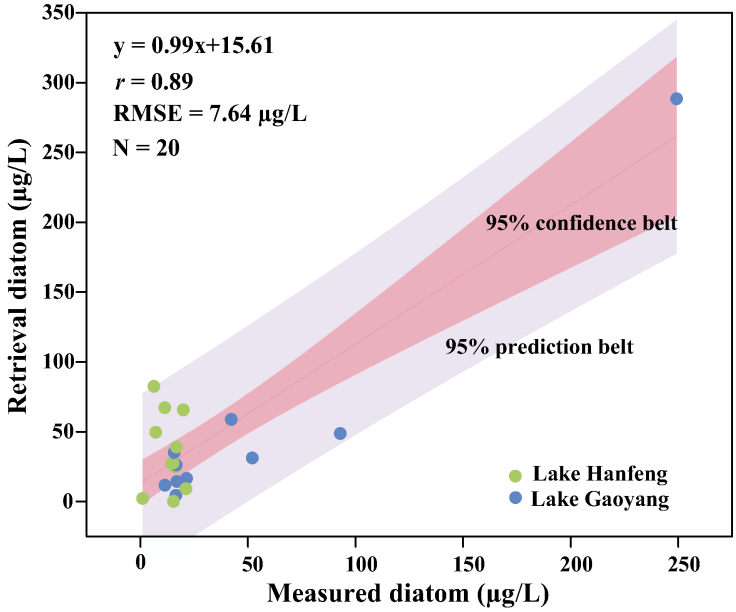



**Figure 4.** Scatter plots indicating contrast between the retrieval and measured diatom concentrations in the typical TGR tributary. N is the sample sum of field observations consistent with satellite observations.

Spatially, the diatom concentration exhibits significant consistency in the typical TGR tributary, with frequent appearances of simultaneous high or low value in Lakes Hanfeng and Gaoyang (Figure 5). Specifically, the inundation areas of the two artificial lakes are almost in yellowish and orangish schemes (moderate diatom concentration). Lakes Hanfeng and Gaoyang primarily exist in a greenish scheme (low diatom concentration) between July and August. Subsequently, yellowish and orangish schemes have been rebuilt synchronously in most of the zones of these two artificial lakes until the onset of winter. It is important that a reddish scheme (high diatom concentration) mainly appears along the sub-thalweg line near the outlet of Lake Gaoyang during the spring, rather than enriching in the backwater bay and nearshore waters during other seasons. Overall, the diatom concentration in Lake Hanfeng is not significantly higher than that in Lake Gaoyang, indicating that diatoms can at least adapt to the strong fluidity.

According to the diatom concentration time series during 2019–2023, it can be seen that there were 10, 4, and 11 instances where the diatom concentration exceeded 10 µg/L (i.e., diatom bloom occurrence) in the Xiaojiang River, upstream Lake Hanfeng, and downstream Lake Gaoyang, respectively (Figure 6). The results obtained for different cross-sections of the typical TGR tributary with similar meteorological conditions further confirm that diatoms do not necessarily prefer relatively static hydrological conditions. It is worth noting that diatom blooms occurred throughout the entire TGR tributary in the spring of 2022 before the record-breaking summer heatwave in the Yangtze River Basin, indicating that diatoms can adapt to air temperatures of 25–30 °C and discomfort at sustained high air temperatures (greater than 40 °C).

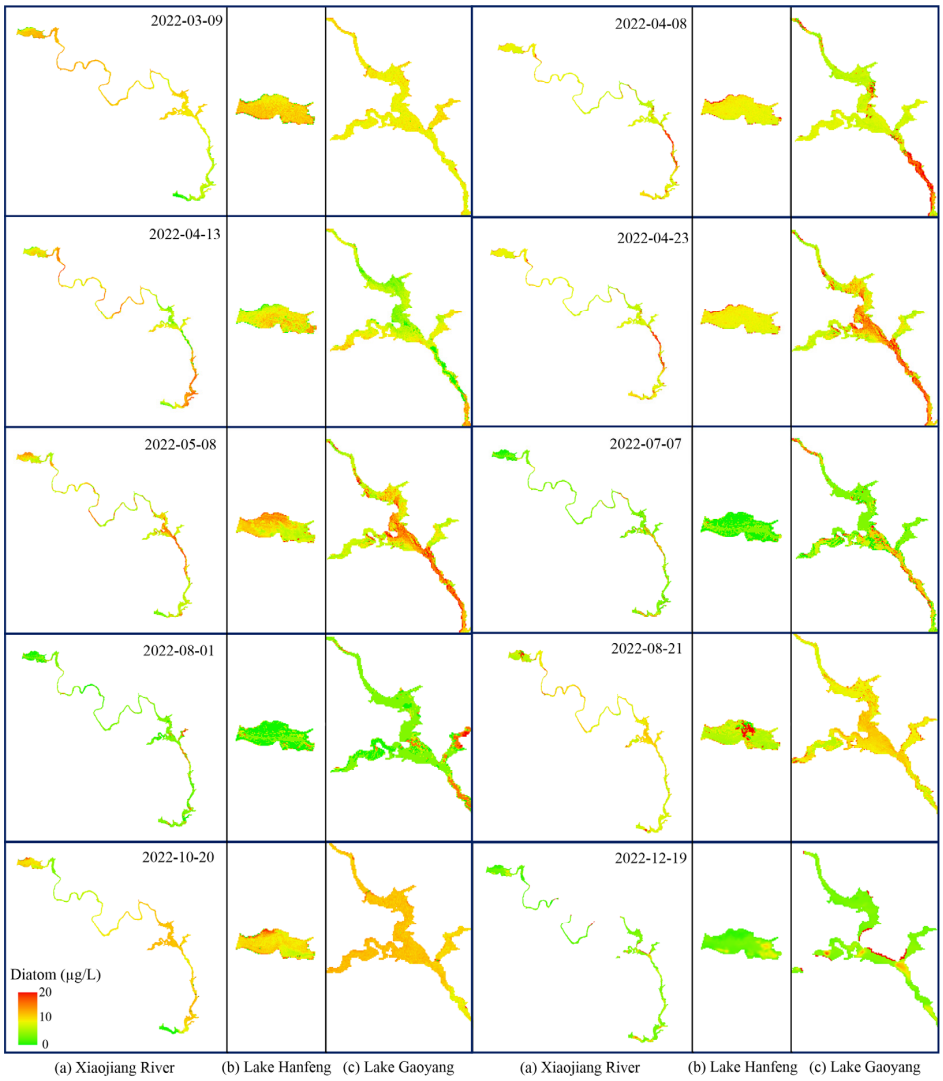



**Figure 5.** Diatom distribution examples in (**a**) the Xiaojiang River, (**b**) upstream Lake Hanfeng, and (**c**) downstream Lake Gaoyang through a hydrological year.

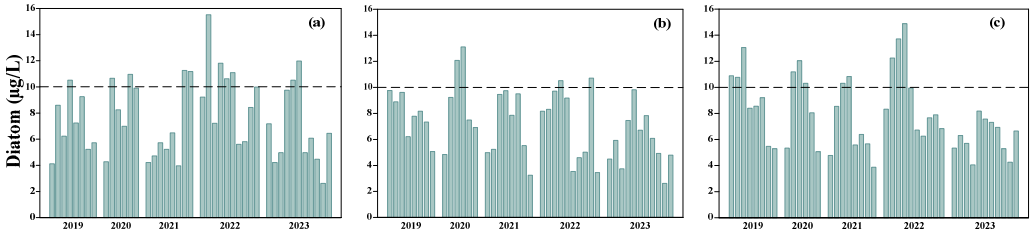



**Figure 6.** Time series of mean diatom concentrations in (**a**) the Xiaojiang River, (**b**) upstream Lake Hanfeng, and (**c**) downstream Lake Gaoyang from 2019 to 2023. The horizontal dashed line indicates the threshold of diatom bloom occurrence, i.e., diatom concentration = 10 μg/L.

The monthly mean diatom concentrations in different cross-sections of the typical TGR tributary shows a distinct seasonal pattern accompanied by a unified declining trend (Figure 7). Overall, the monthly diatom trend in the Xiaojiang River exhibits a bimodal feature, with the spring peak emerging in April–May and the summer peak emerging in July–August (Figure 7a). Based on the premise of the bimodal feature, the summer peak of the upstream Lake Hanfeng exhibits a sub-bimodal feature, while the downstream Lake Gaoyang presents a sub-bimodal feature in spring, as shown in Figure 7b,c. Furthermore,

compared with the entire TGR tributary, the monthly diatom trends in the upstream Lake Hanfeng and downstream Lake Gaoyang are more dramatic, according to the distance between the diatom peak and valley. More importantly, the spring diatom bloom (diatom concentration $\geq$ 10 μg/L) has become a normalized occurrence during the past five years in the two artificial lakes.

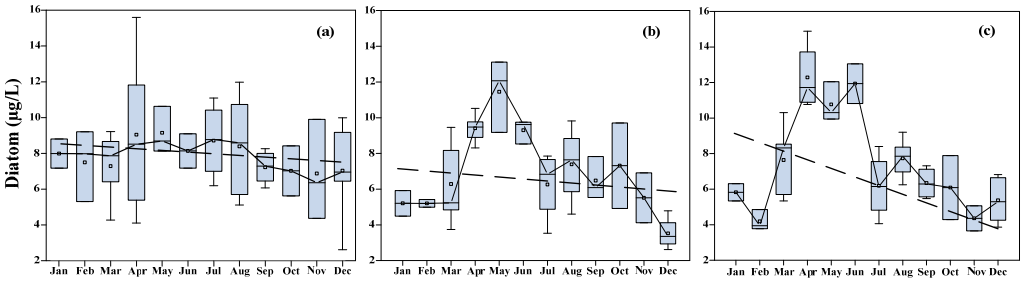



**Figure 7.** Boxplots for monthly mean diatom concentrations in (**a**) the Xiaojiang River, (**b**) upstream Lake Hanfeng, and (**c**) downstream Lake Gaoyang from 2019 to 2023. The dashed lines denote the monthly diatom trends, and the solid lines connect the monthly mean diatom concentrations.

The yearly mean diatom concentrations in the Xiaojiang River, upstream Lake Hanfeng, and downstream Lake Gaoyang during 2019–2023 display a similar declining trend (Figure 8). Specifically, the three yearly diatom trend lines point to 7–8 μg/L, with the discrepancies being the change rates of −0.06, −0.43, and −0.38, suggesting that different cross-sections of the typical TGR tributary are currently in the process of decelerated, accelerated, and stable improvement in controlling diatom blooms, respectively. Synchronously, the Xiaojiang River, upstream Lake Hanfeng, and downstream Lake Gaoyang present relatively high diatom concentrations in 2020 and 2022, while relatively low diatom concentrations appear in 2021, further proving the consistency among the interannual diatom dynamics.

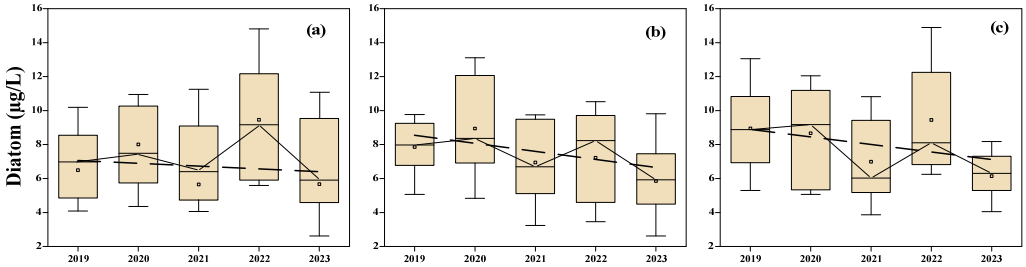



**Figure 8.** Boxplots for yearly mean diatom concentrations in (**a**) the Xiaojiang River, (**b**) upstream Lake Hanfeng, and (**c**) downstream Lake Gaoyang from 2019 to 2023. The dashed lines denote the yearly diatom trends, and the solid lines connect the yearly mean diatom concentrations.

### *3.2. Hydrological and Meteorological Drivers of Diatom Trends*

The relationship between monthly mean diatom concentration and hydrological/meteorological drivers is displayed in Figure 9a. The results show that the declining diatom trend is only dependent on precipitation, with $r = -0.63$, in the Xiaojiang River. Additionally, for the upstream Lake Hanfeng, there is a strong correlation between water level and diatom concentration ($r = -0.62$). By contrast, in downstream Lake Gaoyang, increases in air temperature and sunshine duration as well as decreases in precipitation and water level may accelerate the diatom growth to a limited extent ($|r| < 0.6$). Overall, the monthly diatom trends along the Xiaojiang River present statistically differentiated correlations with the dam construction and local climate.

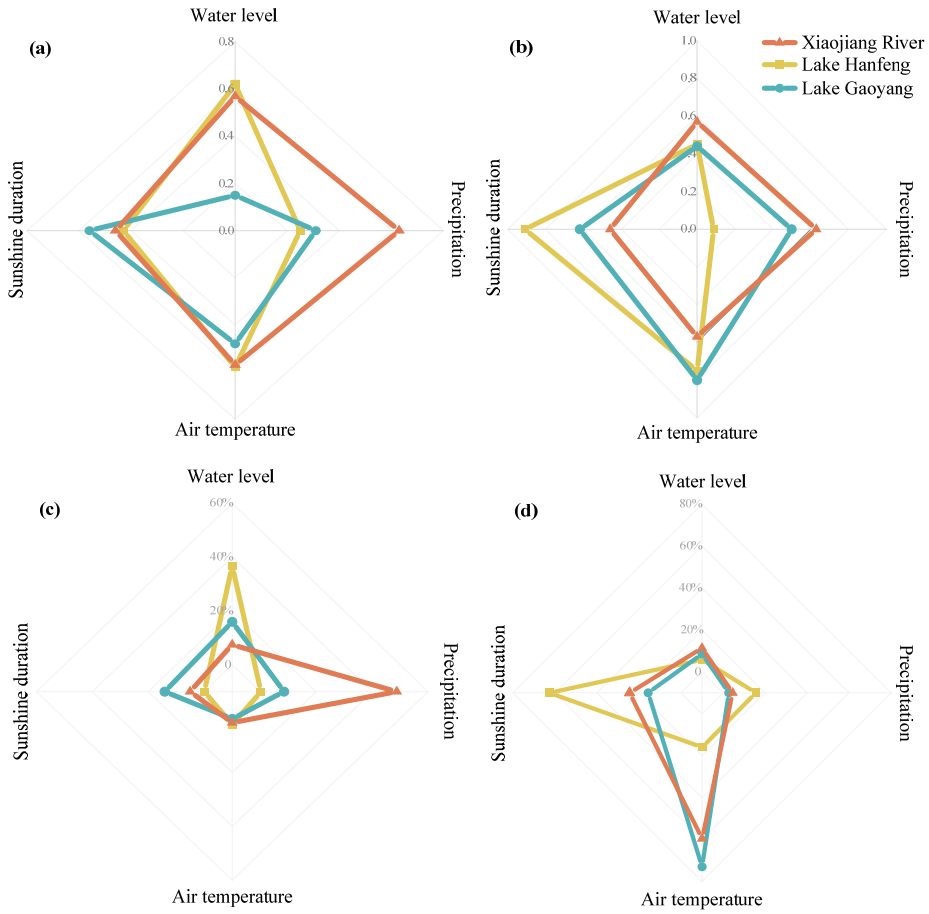



**Figure 9.** Causal correlations between driving factors and absolute values of (**a**) monthly and (**b**) yearly mean diatom concentrations, as well as the relative contributions of driving factors to (**c**) monthly and (**d**) yearly diatom trends.

Figure 9b presents the relationship between yearly mean diatom concentration and hydrological/meteorological drivers. As expected, precipitation appears to have a close correlation with diatom concentration in the Xiaojiang River ($r = -0.64$); moreover, advances in sunshine duration and air temperature can transform the diatom concentration into an accelerated rising in the upstream Lake Hanfeng and downstream Lake Gaoyang, according to the intense positive correlation ($r \geq 0.6$), indicating that the response of yearly diatom trends to the local climate is statistically significant.

Subsequently, a quantitative analysis must be considered for relative contributions of hydrological and meteorological drivers to the declining trend of diatom concentration. Overall, on the monthly and yearly scales, the total contributions of water level, air temperature, sunshine duration, and precipitation to the diatom trends are 0.13%–48.85% and 2.72%–73.01%, with mean values of 11.71% and 24.99%, respectively (Figure 9c,d), indicating a strong temporal heterogeneity in the coupling driver contribution of the declining diatom trend across different cross-sections of the TGR tributary.

Due to the high residual and weak correlation, only precipitation and water level have been found to play dominant roles (contribution = 48.85% and 36.52%; $|r| = 0.63$ and 0.62) in the diatom trends in the Xiaojiang River and upstream Lake Hanfeng on the monthly scale, respectively (Figure 9c). The results may be attributable to other drivers not included in this study controlling the monthly diatom trend. In contrast, on the yearly scale, air temperature plays an important role (contribution = 59.56% and 73.01%) in regulating the diatom trends in the Xiaojiang River and downstream Lake Gaoyang (Figure 9d). Moreover, sunshine duration has a slightly weaker performance (contribution = 62.61%), significantly

impacting the yearly diatom trend in the upstream Lake Hanfeng. Therefore, we conclude that the dam construction and local climate have altered the seasonal and interannual diatom trends across different cross-sections of the TGR tributary studied herein.

## 4. Discussion

### *4.1. Limitations and Uncertainties of Sentinel-Derived Diatom Concentration*

There is still a certain difference between the measured and retrieval diatom concentrations, mainly reflected in a contradiction that the measured value is higher in downstream Lake Gaoyang, while the corresponding retrieval value is higher in upstream Lake Hanfeng (Figure 4). This may be attributed to the disadvantage of satellite observation in terms of accurate computation on a small scale. In addition, the measured diatom concentrations are mostly in a relatively low value range (0–50 μg/L), and the retrieval accuracy for high diatom concentrations still needs to be validated. For the phytoplankton community in the freshwater ecosystem, cyanobacteria and green algae are still the dominant species, with few stable phytoplankton communities dominated by diatoms [46]. Thus, it is unknown whether the Sentinel-derived diatom concentration is applicable to all rivers, lakes, and reservoirs.

In future research, this method will extend to more diatom abundance types and modeling frameworks for developing the potential performance and overcome the application limitation in more freshwater ecosystems. Additionally, due to the influence of cloudy and foggy weather around the TGR, the temporal density of Sentinel-2 MSI imagery is insufficient, which may lead to misjudging the temporal trend of diatom concentration; therefore, according to the narrow channel of the TGR's tributaries, multi-source remote sensing data with a spatial resolution surpassing 30 m (such as Landsat, Gaofen, and Huanjing imagery) should be fully included. Considering the impact of atmospheric correction algorithms on water color remote sensing, the ACOLITE algorithm should be suggested to pretreat the satellite imagery, comparing the effects of different atmospheric correction algorithms on the spatiotemporal analysis results of diatom dynamics, to further improve the diatom concentration retrieval accuracy in the TGR's tributaries.

### *4.2. Implications for Reservoir Management*

Compared with conventional site-specific sampling approaches, the Sentinel-derived diatom concentration allows for a more accurate evaluation of diatom dynamics in the typical TGR tributary, and therefore has two implications for reservoir management.

First, the SVD-based retrieval model of diatom concentration proposed herein can greatly aid managers in formulating a valid strategy for restraining harmful cyanobacterial blooms. The Sentinel-derived diatom concentration can determine whether dominant algae are harmful during the bloom period. Specifically, if the diatom concentration in the phytoplankton community is greater than 10 μg/L, it indicates that the diatom occupies a dominant position, and harmful cyanobacteria are inevitably at a disadvantage; if the diatom concentration is less than 10 μg/L, it suggests that the diatom is in a disadvantaged state, and in such cases, harmful cyanobacteria may dominate the phytoplankton community during the bloom periods. Our goal is to control the water level by adjusting the Wuyang and Three Gorges Dams, exploring a balance with local climate to prevent the dominant species being transformed completely from diatom to cyanobacteria. Thus, along with local warming in the Yangtze River Basin, determining how to avoid the harmful cyanobacterial bloom has been an urgent issue for reservoir managers.

Second, the SVD-based retrieval model suggests an effective method for early warnings of harmless diatom blooms, eliminating ship oil spills, because the water color of diatom blooms is similar to that of ship oil spills, as shown in Figure 10. At present, no approach exists that can be applied to reveal the diatom dynamics within a large reser-

voir [47]. In the present study, the SVD-based retrieval model can provide large-scale diatom concentration information, allowing us to gain new insights into harmless diatom bloom occurrence to reduce the unnecessary costs of oil leakage disposal. Although the retrieval model of diatom concentration is proposed in the TGR tributary, we believe that this model can serve as a case study that describes the benefits of using Sentinel-derived diatom concentration to confirm harmless algal blooms and exclude ship oil spills in advance.




**Figure 10.** Comparative examples between field photographs of (**a**) harmless diatom bloom (Lake Gaoyang in April 2023) and (**b**) ship oil spill (Rotterdam, The Netherlands, in April 2019).

## 5. Conclusions

The spatial distribution and temporal trend of diatom concentration in the primary TGR tributary from 2019 to 2023 were investigated using the SVD-based retrieval model. Although there are many discrepancies in hydrology, geomorphology, and other environmental conditions between the upstream Lake Hanfeng and downstream Lake Gaoyang, a general declining trend in diatom concentration on the different temporal scales was detected. The statistical analysis indicates that water level, air temperature, sunshine duration, and precipitation can illustrate the seasonal and interannual diatom trends to some extent, indicating that dam construction and local climate play different roles in controlling diatom blooms. This study offers new insights into tracking diatom dynamics for reservoir managers, geographers, and limnologists.

**Author Contributions:** M.G. and L.F. (Lei Feng) were responsible for writing—original manuscript, data collection, model training, and processing analysis; J.S. and B.Z. were responsible for the manuscript revision and research design; Y.W. and L.W. contributed to the platform construction and imager adjustment; L.F. (Li Feng) and M.L. contributed to the formal analysis and image processing. All authors have read and agreed to the published version of the manuscript.

**Funding:** This study was conducted with the support of the National Natural Science Foundation of China (U22A20561 and 42371326) and Chongqing Natural Science Foundation (cstc2022jcyj-msxmX0648).

**Data Availability Statement:** The data are available from the corresponding author on reasonable request.

**Acknowledgments:** The authors would like to thank Jianrong Ma, Zhaofei Wen, and Jie Wu for their help in the field sample collection and experimental analysis.

**Conflicts of Interest:** The authors declare no conflicts of interest.

## References

1. Falkowski, P.G.; Barber, R.T.; Smetacek, V. Biogeochemical controls and feedbacks on ocean primary productivity. *Science* **1998**, *281*, 200–206. [CrossRef] [PubMed]
2. Field, C.B.; Behrenfeld, M.J.; Randerson, J.T.; Falkowski, P. Primary production of the biosphere: Integrating terrestrial and oceanic components. *Science* **1998**, *281*, 237–240. [CrossRef] [PubMed]
3. Behrenfeld, M.J.; Falkowski, P.G. Photosynthetic rates derived from satellite-based chlorophyll concentration. *Limnol. Oceanogr.* **1997**, *42*, 1–20. [CrossRef]

4. Gameiro, C.; Cartaxana, P.; Brotas, V. Environmental drivers of phytoplankton distribution and composition in Tagus Estuary, Portugal. Estuar. *Coastal Shelf S.* **2007**, *75*, 21–34. [CrossRef]
5. Wurtsbaugh, W.A.; Paerl, H.W.; Dodds, W.K. Nutrients, eutrophication and harmful algal blooms along the freshwater to marine continuum. *Wires. Water* **2019**, *6*, e1373. [CrossRef]
6. Arrigo, K.R. Marine microorganisms and global nutrient cycles. *Nature* **2005**, *437*, 349–355. [CrossRef] [PubMed]
7. Round, F.E. *The Diatoms: Biology and Morphology of the Genera*; Cambridge University Press: Cambridge, UK, 1990.
8. Le Quéré, C.; Harrison, S.P.; Prentice, I.C.; Buitenhuis, E.T.; Aumont, O.; Bopp, L.; Claustre, H.; Da Cunha, L.C.; Geider, R.; Giraud, X.; et al. Ecosystem dynamics based on plankton functional types for global ocean biogeochemistry models. *Glob. Chang. Biol.* **2005**, *11*, 2016–2040. [CrossRef]
9. Faucci, A.; Philippoff, J.; Veresan, C. The Microscopic World of Plankton. *Sci. Scope* **2019**, *42*, 51–61. [CrossRef]
10. Taurozzi, D.; Cesarini, G.; Scalici, M. Diatoms as bioindicators for health assessments of ephemeral freshwater ecosystems: A comprehensive review. *Ecol. Indic.* **2024**, *166*, 112309. [CrossRef]
11. Ren, J.; Zhou, T.; Zhu, G.W.; Jin, Y.W.; Cui, Y.; Xu, H.; Zhu, M.Y. Characteristics of diatom community structure and its controlling factors in Sunan Reservoir. *Environ. Sci.* **2016**, *37*, 1742–1753.
12. Kramer, S.J.; Roesler, C.S.; Sosik, H.M. Bio-optical discrimination of diatoms from other phytoplankton in the surface ocean: Evaluation and refinement of a model for the Northwest Atlantic. *Remote Sens. Environ.* **2018**, *217*, 126–143. [CrossRef]
13. Mann, D.G. The species concept in diatoms. *Phycologia* **1999**, *38*, 437–495. [CrossRef]
14. Desrosiers, C.; Leflaive, J.; Eulin, A.; Ten-Hage, L. Bioindicators in marine waters: Benthic diatoms as a tool to assess water quality from eutrophic to oligotrophic coastal ecosystems. *Ecol. Indic.* **2013**, *32*, 25–34. [CrossRef]
15. Zhu, G.W.; Jin, Y.W.; Ren, J.; Xia, M.F.; Xu, H.; Zhu, M.Y.; Fei, G.S. Characteristics and countermeasures of diatom blooms in reservoir-type water source areas of Taihu Lake Basin. *J. Lake Sci.* **2016**, *28*, 9–21.
16. Mackey, M.D.; Mackey, D.J.; Higgins, H.W.; Wright, S.W. CHEMTAX—A program for estimating class abundances from chemical markers: Application to HPLC measurements of phytoplankton. *Mar. Ecol. Prog. Ser.* **1996**, *144*, 265–283. [CrossRef]
17. Kim, H.; Menden-Deuer, S. Reliability of rapid, semi-automated assessment of plankton abundance, biomass, and growth rate estimates: Coulter Counter versus light microscope measurements. *Limnol. Oceanogr.-Meth.* **2013**, *11*, 382–393. [CrossRef]
18. Haberkorn, I.; Off, C.L.; Besmer, M.D.; Buchmann, L.; Mathys, A. Automated online flow cytometry advances microalgal ecosystem management as in situ, high-temporal resolution monitoring tool. *Front. Bioeng. Biotech.* **2021**, *9*, 642671. [CrossRef]
19. Steinberg, M.K.; First, M.R.; Lemieux, E.J.; Lisa, A.; Drake, L.A.; Nelson, B.N.; Kulis, D.K.; Anderson, D.M.; Welschmeyer, N.A.; Herring, P.R. Comparison of techniques used to count single-celled viable phytoplankton. *J. Appl. Phycol.* **2012**, *24*, 751–758. [CrossRef]
20. Shi, W.B.; Tao, Y.; Zhang, X.H. Research on early warning and control technology of diatom bloom in water environment. *Water Resour. Hydropower Eng.* **2015**, *46*, 60–63.
21. Shi, K.; Zhang, Y.L.; Qin, B.Q.; Zhou, B.T. Remote sensing of cyanobacterial blooms in inland waters: Present knowledge and future challenges. *Sci. Bull.* **2019**, *64*, 1540–1556. [CrossRef]
22. Markogianni, V.; Kalivas, D.; Petropoulos, G.P.; Dimitriou, E. Estimating chlorophyll-a of inland water bodies in Greece based on landsat data. *Remote Sens.* **2020**, *12*, 2087. [CrossRef]
23. Cetinić, I.; Rousseaux, C.S.; Carroll, I.T.; Chase, A.P.; Kramer, S.J.; Werdell, J.P.; Siegel, D.A.; Dierssen, H.M.; Catlett, D.; Neeley, A.; et al. Phytoplankton composition from space: Requirements, opportunities, and challenges. *Remote Sens. Environ.* **2024**, *302*, 113964. [CrossRef]
24. Sun, D.Y.; Chen, Y. H, Liu, J.Q.; Liu, J.Q.; Wang, S.Q.; He, Y.J. Preliminary study on the application of HY-1C/D satellite data for phytoplankton remote sensing. *J. Remote Sens.* **2023**, *27*, 128–145.
25. Chen, Y.H.; Sun, D.Y.; Chen, W.W.; Fan, J.; Wang, S.Q.; Zhang, H.L.; He, Y.J. Research on inversion model of diatom concentration in coastal waters based on singular value decomposition technology. *Mar. Sci.* **2022**, *46*, 25–35.
26. Xiao, W.; Huang, Y.; Mi, W.; Wu, H.; Bi, Y. Variation of diatoms and silicon in a tributary of the Three Gorges Reservoir: Evidence of interaction. *Water* **2019**, *11*, 1369. [CrossRef]
27. Huang, Y.; Mi, W.; Hu, Z.; Bi, Y. Effects of the Three Gorges Dam on spatiotemporal distribution of silicon in the tributary: Evidence from the Xiangxi River. *Environ. Sci. Pollut. R.* **2019**, *26*, 4645–4653. [CrossRef]
28. Zhou, B.; Hu, J.; Chen, L.; Yuan, Y.; Yang, X.; Hu, Z.; Bi, Y. Spatio-temporal patterns of diatom communities in front of the Three Gorges Dam: Evidence of the effects of hydrodynamics. *Fresenius Environ. Bull.* **2015**, *24*, 2593–2602.
29. Ji, L.L.; Zhao, L.; Ouyang, T.; Yang, S.Q.; Zheng, B.H.; Du, Y.X. Impact and driving effect of environmental heterogeneity on the epiphytic diatom community in Xiangxi River, a tributary of the Three Gorges Reservoir. *Environ. Sci.* **2023**, *44*, 2083–2092.
30. Yang, Z.J.; Wei, C.Y.; Liu, D.F.; Lin, Q.C.; Huang, Y.L.; Wang, C.F.; Ji, D.B.; Ma, J.; Yang, H. The influence of hydraulic characteristics on algal bloom in three gorges reservoir, China: A combination of cultural experiments and field monitoring. *Water Res.* **2022**, *211*, 118030. [CrossRef]

31. Xiao, Y.; Li, Z.; Guo, J.S.; Fang, F.; Smith, V.H. Succession of phytoplankton assemblages in response to large-scale reservoir operation: A case study in a tributary of the Three Gorges Reservoir, China. *Environ. Monit. Assess.* **2016**, *188*, 153. [CrossRef]
32. Zhou, B.T.; Shang, M.S.; Feng, L.; Shan, K.; Feng, L.; Ma, J.R.; Liu, X.N.; Wu, L. Long-term remote tracking the dynamics of surface water turbidity using a density peaks-based classification: A case study in the Three Gorges Reservoir. China. *Ecol. Indic.* **2020**, *116*, 106539. [CrossRef]
33. Li, Z.; Wang, S.; Guo, J.S.; Fang, F.; Gao, X.; Long, M. Responses of phytoplankton diversity to physical disturbance under manual operation in a large reservoir, China. *Hydrobiologia* **2012**, *684*, 45–56. [CrossRef]
34. Xiang, R.; Wang, L.J.; Li, H.; Tian, Z.B.; Zheng, B.H. Water quality variation in tributaries of the Three Gorges Reservoir from 2000 to 2015. *Water Res.* **2021**, *195*, 116993. [CrossRef] [PubMed]
35. Zhou, B.T.; Shi, K.; Wang, W.J.; Zhang, D.; Qin, B.Q.; Zhang, Y.L.; Dong, B.L.; Shang, M.S. Phytoplankton succession phenology trends in the backwaters of the three gorges reservoir in China and their drivers: Results from satellite observations. *Ecol. Indic.* **2022**, *143*, 109435. [CrossRef]
36. Liu, L.; He, X.Y.; Fu, J.K.; Yang, Y.J.; Mi, W.M.; Shi, J.Q.; Wu, Z.X. Benthic diatom communities in the main stream of three gorges reservoir area and its relationship with environmental factors. *Environ. Sci.* **2019**, *40*, 3577–3587.
37. Jankowiak, J.; Hattenrath-Lehmann, T.; Kramer, B.J.; Ladds, M.; Gobler, C.J. Deciphering the effects of nitrogen, phosphorus, and temperature on cyanobacterial bloom intensification, diversity, and toxicity in western Lake Erie. *Limnol. Oceanogr.* **2019**, *64*, 1347–1370. [CrossRef]
38. Brian, A.W.; Malcolm, P. *The Ecology of Cyanobacteria: Their Diversity in Time and Space*; Kluwer Academic Publishers: New York, NY, USA, 2002.
39. Hu, H.; Wei, Y. *The Freshwater Algae of China: Systematics, Taxonomy and Ecology*; Science Press: Beijing, China, 2006.
40. Mobley, C.D. Estimation of the remote-sensing reflectance from above-surface measurements. *Appl. Opt.* **1999**, *38*, 7442–7455. [CrossRef]
41. Gernez, P.; Lafon, V.; Lerouxel, A.; Curti, C.; Lubac, B.; Cerisier, S.; Barillé, L. Toward Sentinel-2 high resolution remote sensing of suspended particulate matter in very turbid waters: SPOT4 (take5) experiment in the Loire and Gironde estuaries. *Remote Sens.* **2015**, *7*, 9507–9528. [CrossRef]
42. Zhu, Z.; Wang, S.X.; Woodcock, C.E. Improvement and expansion of the fmask algorithm: Cloud, cloud Shadow, and snow detection for Landsats 4-7, 8, and Sentinel 2 images. *Remote Sens. Environ.* **2015**, *159*, 269–277. [CrossRef]
43. Xi, H.Y.; Losa, S.N.; Mangin, A.; Soppa, M.A.; Garnesson, P.; Demaria, J.; Liu, Y.Y.; d'Andon, O.H.F.; Bracher, A. Global retrieval of phytoplankton functional types based on empirical orthogonal functions using CMEMS GlobColour merged products and further extension to OLCI data. *Remote Sens. Environ.* **2020**, *240*, 111704. [CrossRef]
44. Bracher, A.; Taylor, M.H.; Taylor, B.; Dinter, T.; Röttgers, R.; Steinmetz, F. Using empirical orthogonal functions derived from remotesensing reflectance for the prediction of phytoplankton pigment concentrations. *Ocean. Sci.* **2015**, *11*, 139–158. [CrossRef]
45. Fan, J.; Sun, D.Y.; Wang, S.Q.; Zhang, H.L.; Huan, Y.; He, Y.J. Inversion model of diatoms concentration in coastal water based on absorption coefficients. *J. Remote Sens.* **2023**, *27*, 363–375. [CrossRef]
46. Wright, S.W.; van den Enden, R.L.; Pearce, I.; Davidson, A.T.; Scott, F.J.; Westwood, K.J. Phytoplankton community structure and stocks in the Southern Ocean (30–80° E) determined by CHEMTAX analysis of HPLC pigment signatures. *Deep. Sea Res. Part II: Top. Stud. Oceanogr.* **2010**, *57*, 758–778. [CrossRef]
47. Shang, S.L.; Wu, J.Y.; Huang, B.Q.; Lin, G.; Lee, Z.P.; Liu, J.; Shang, S.P. A new approach to discriminate dinoflagellate from diatom blooms from space in the East China Sea. *J. Geophys. Res. Oceans* **2014**, *119*, 4653–4668. [CrossRef]


**Disclaimer/Publisher's Note:** The statements, opinions and data contained in all publications are solely those of the individual author(s) and contributor(s) and not of MDPI and/or the editor(s). MDPI and/or the editor(s) disclaim responsibility for any injury to people or property resulting from any ideas, methods, instructions or products referred to in the content.